Civil Engineering Infrastructures Journal, 48(2): 285-296, December 2015
ISSN: 2322-2093

Evaluating the Seismic Performance of Steel-SMA Hybrid Braces

Hooshmand, M.[1], Rafezy, B.[2], Hosseinzadeh, Y.[3] and Ahmadi, H.[4*]

[1] M.Sc. Graduate, Young Researchers and Elite Club, Tabriz Branch, Islamic Azad University, Tabriz, Iran

[2] Associate Professor, Department of Civil Engineering, Sahand University of Technology, Tabriz, Iran

[3] Associate Professor, Faculty of Civil Engineering, University of Tabriz, Tabriz, Iran

[4] Assistant Professor, Faculty of Civil Engineering, University of Tabriz, Tabriz, Iran

Received: 21 Apr. 2014 Revised: 02 Feb. 2015 Accepted: 10 Feb. 2015

Abstract: The seismic performance of hybrid braces composed of steel and shape memory alloy (SMA) was investigated in this paper. Six types of hybrid braces were used, constituted by SMA content of 0, 20, 40, 60, 80, and 100%. A nonlinear dynamic analysis was performed under El Centro earthquake records, with the maximum acceleration of 0.6*g* and 0.9*g*. Our results showed that the seismic performance, i.e., the amount of energy absorption and residual strain, of steel–SMA hybrid braces depends on the SMA content. The optimal value of SMA content was 20%, as, at this concentration, a hybrid brace can be designed with good seismic performance at a justifiable fabrication cost.

Keywords: Finite Element modeling, Hybrid brace, Nonlinear dynamic analysis, Seismic performance, Shape Memory Alloy (SMA)

INTRODUCTION

Smart systems in structural engineering can automatically adapt in response to unexpected loading to provide the structure with the features of safety, longevity, and efficiency. A recent technology offers the possibility of achieving these goals through the production and development of smart materials. Shape memory alloys (SMAs) have been used since more than a decade as smart materials in structural and earthquake engineering (Mansouri, 2008).

In recent years, several studies have been conducted on SMA applications in civil engineering; for example, in seismic isolation systems (Alvandi and Ghassemieh, 2014; Ozbulut and Hurlebaus, 2011), in energy dissipation systems (Ma and Yam, 2011; Motahari et al., 2007), in dampers for bridges (Mekki and Auricchio, 2011; Padgett et al., 2009), and for retrofitting masonry and historical structures (Shrestha et al., 2011). SMAs have also been studied for use in concrete structures such as reinforcing bars (Malagisi et al., 2014; Billah and Alam, 2012; Youssef and Elfeki, 2012), in structural joints (Speicher et al., 2011; Yam et al., 2014), and in dams (Sun, 2011).

One of the most important and effective applications of SMAs in civil engineering is their use as braces, owing to their superelasticity and shape memory properties. SMAs can regain the original state to provide considerable energy dissipation (Asgarian and Moradi, 2011; Miller et al., 2012; Yang et al., 2010).

Although the studies on SMA application in civil engineering have increased recently, there use in the structural systems remains limited. One of the reasons for this is the

*Corresponding author E-mail: h-ahmadi@tabrizu.ac.ir

high cost of these alloys. In this study, we investigated the efficiency of SMAs in hybrid braces. This study investigated the seismic performance and the economic justification of typical frame bracing systems composed of steel and SMA by suggesting the optimal content of SMA. Considering the difference between the cost of steel and SMA, it is essential to determine the amount of SMA for use along with steel in a hybrid brace such that a compromise can be reached between the cost of brace and its seismic performance.

SHAPE MEMORY ALLOYS (SMAs)

SMAs have special properties that make distinct from other alloys and metals. Properties of SMAs such as shape memory and super elasticity are described in this section.

Shape Memory Properties

One-Way Shape Memory Effect

Normally, the SMAs are in twinned martensite phase. Applying stress turns twinned martensite into detwinned martensite. In this way, the alloy does not return to its original form and, consequently, the residual strains are generated in the sample. Heating of the alloy to a temperature above the critical value results into a phase change into austenite, in which the residual strain disappears and the alloy returns to its initial state. This mode is shown in Figure 1.

Two-Way Shape Memory Effect

In two-way shape memory effect, which is similar to one-way shape memory effect, SMAs remain in the martensite phase at the room temperature. In this case, without applying any stress and only through heating and cooling, the samples showed a change from the austenite to the martensite phase and vice versa. The alloy can memorize these two forms at high and low temperatures. In order to achieve the two-way shape memory effect, the training method should be used. This property is used in the production of reversible bolts, stimulators that are sensitive to temperature, and medical inter-plantings (Auricchio et al., 2006). This mode is shown in Figure 2.

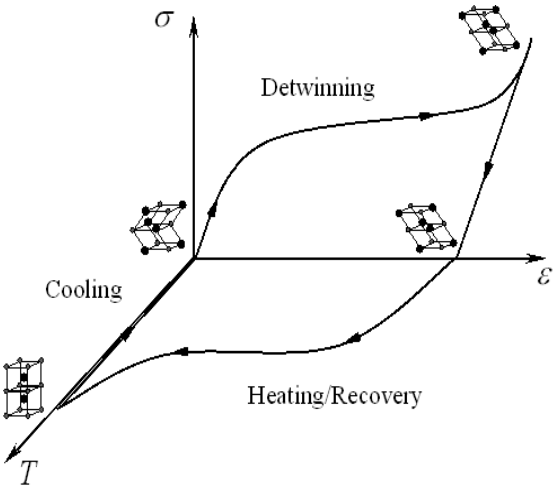

Fig. 1. Stress–strain diagram in a one-way shape memory effect.

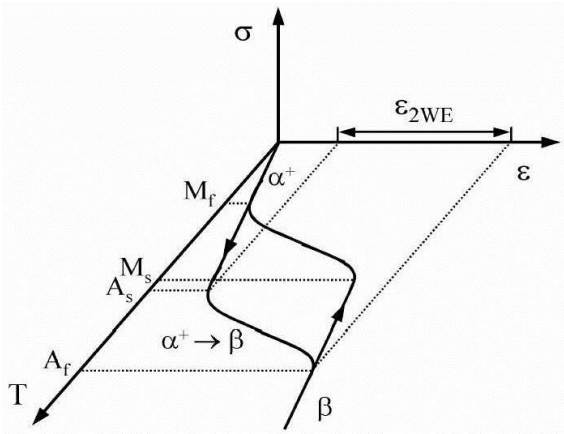

Fig. 2. Stress–strain diagram of the SMA in two-way shape memory effect

Superelastic Properties

In the super elastic mode, the SMA is in the austenite phase. On applying stress, the austenite phase transforms to a stress-induced martensite phase. On unloading the regime, the reverse transformation occurs from the martensite to the austenite phase and, as a result, the material returns to its primary state and does not leave any residual strain. Figure 3 depicts the super elastic behavior of the SMA.

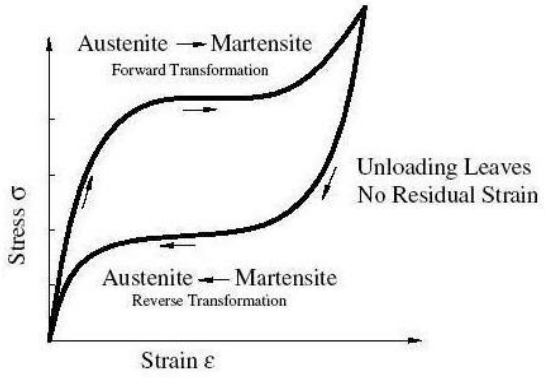

Fig. 3. Stress–strain diagram of the SMA in the superelastic mode (Auricchio et al., 2006)

METHODS

The aim of the present paper was to develop a hybrid brace of steel and SMA that is not only economically justifiable but also has a good seismic performance. To evaluate the seismic behavior of the bracing system, the remaining structural displacement and the structure's energy absorption were used as the basis for the comparison of different studied models.

The price of steel is approximately 0.63$/Kg. The price of SMA used in the present study was approximately 45$/kg; this type of SMA is produced in the Sahand University of Technology, Iran. Hence, the price of SMA is approximately 70 times that of steel. Therefore, considering the great difference between the cost of steel and SMA, it is essential to determine a reasonable amount of SMA to be used along with steel in a hybrid brace such that a compromise can be achieved between the cost of brace and its seismic performance. Neutral atmosphere-welding technology can be used to attach the SMA and steel to fabricate a hybrid brace. Moreover, since the price of construction material fluctuates with time, especially in Iran, in the present study we compared the amount of SMA content and not its cost in different models.

Finite Element Modeling (FEM) and Verification

The FEM-based software package ANSYS v11 was used for modeling and analysis. The verification was performed using a model of braced steel structure that was analyzed with AIMS software (Ghassemiyeh and Kari, 2008). A three-story structure designed by Sabelli (2001) was considered for verification study. Assuming symmetry in the plan, a two-dimensional frame of the structure was analyzed. The height of each floor was 3.96 m and the construction plan was 9.14×9.14 m. Ceilings were built with composite sections, in which the height of steel part and concrete covered 76 mm and 50 mm, respectively. The geometry and sections designed for this frame are described in Table 1 and Figure 4. The SMA braces in each category had axial stiffness and axial force (σ_A, σ and A denote stress and section area, respectively) identical to the Buckling-Resistance Braces (BRBs). Notably, the axial deformation of the beam was ignored (Ghassemiyeh and Kari, 2008).

Table 1. Geometrical properties used in Sabelli's model (Ghassemiyeh and Kari, 2008)

Story	Braces	Beams	Columns
1	HSS 8x8x0.5	W 18X46	W 12X106
2	HSS 6x6x0.5	W 18X46	W 12X106
3	HSS 5x5x0.375	W 18X46	W 12X106

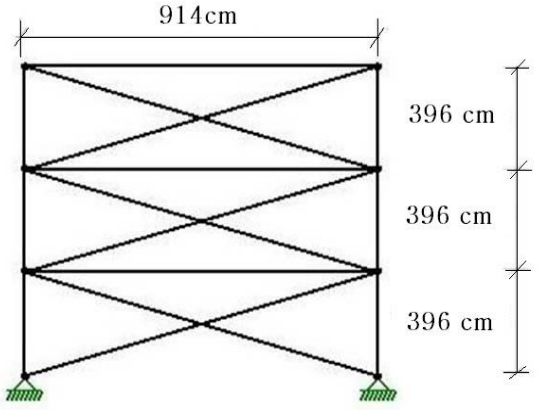

Fig. 4. Geometrical model of the structure (Ghassemiyeh and Kari, 2008)

The elasticity modulus, plastic modulus, and the yield stress of steel members were considered 200000, 20000, and 240 MPa, respectively; and the damping ratio was considered as 0.05. The mechanical properties of superelastic SMA cross-braces have been specified in Table 2 (Ghassemiyeh and Kari, 2008). The stress–strain curve of SMA is corresponding to the alloy produced in the Sahand University of Technology, Iran. The strain hardening slope for SMA stress–strain diagram was selected based on the respective laboratory results. An equal strain-hardening slope was also assumed for the steel stress– strain diagram.

Table 2. Parameters used in the behavioral model of SMA (Ghassemiyeh and Kari, 2008)

Yield Stress	Value
Martensite-to-Austenite start stress	420 MPa
Martensite-to-Austenite finish stress	500 MPa
Austenite-to-Martensite start reverse stress	300 MPa
Austenite-to-Martensite finish reverse stress	200 MPa
Phase transformation strain	6.5%
Martensite-to-Austenite modulus of Elasticity	40000 MPa

It is assumed that the behavior of SMA under tensile force is identical to its behavior under a compressive load. In order to avoid the in-plane buckling, brace section was selected during the FE modeling of the brace, such that its slenderness coefficient was small enough to prevent any buckling. Out-of-plane buckling was also avoided by using lateral restraints normal to the brace plane.

Only two models of Ghassemiyeh and Kari (2008) were used for the verification study. These models were analyzed under the El-Centro earthquake, with an acceleration of 0.6*g*. The first model had a steel buckling-resistance brace (BRB) and the second model had an SMA brace. A comparison of the results of Ghassemiyeh and Kari (2008) with those of the present numerical study is depicted in Figures 5−10. The post-buckling behavior of the brace was not investigated in the present study.

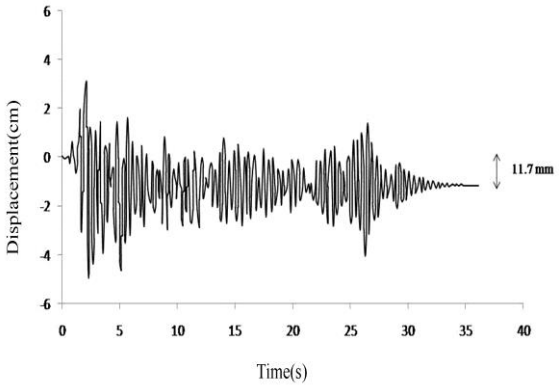

Fig. 5. The time history of the horizontal displacement of the third floor level in the BRB system obtained by Ghassemiyeh and Kari (2008)

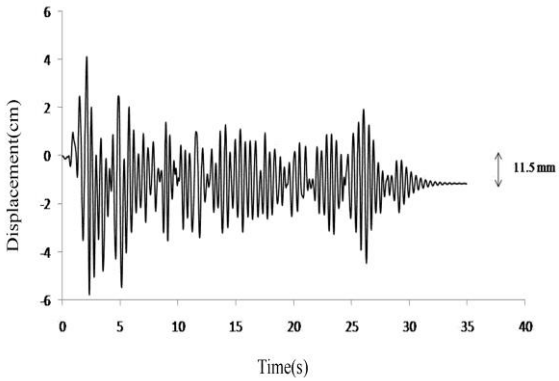

Fig. 6. The time history of the horizontal displacement of the third floor level in the BRB system obtained from the present numerical study with ANSYS

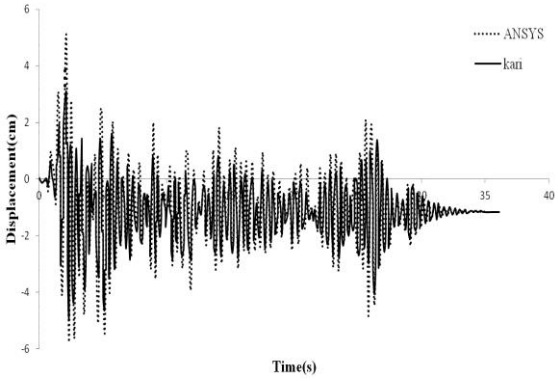

Fig. 7. Comparison of the time history of the third floor level horizontal displacement in the BRB system obtained from the present numerical study with the results of Ghassemiyeh and Kari (2008)

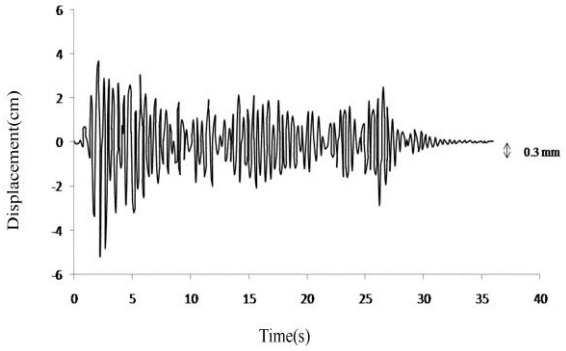

Fig. 8. The time history of the horizontal displacement of the third floor level in the SMA bracing system obtained by Ghassemiyeh and Kari (2008)

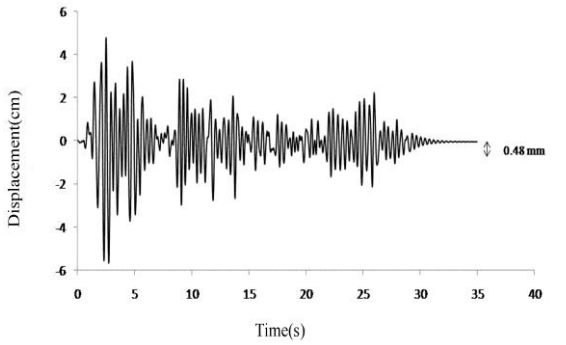

Fig. 9. The time history of the horizontal displacement of the third floor level in the SMA bracing system of the present numerical study with ANSYS

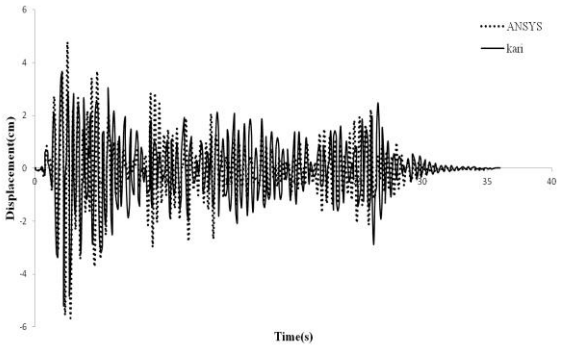

Fig. 10. Comparison of the time history of the third floor level horizontal displacement in the SMA bracing system of the present numerical study with the results of Ghassemiyeh and Kari (2008)

As observed in Figures 5-10, a reasonable agreement was noted between the diagrams of Ghassemiyeh and Kari (2008) and the ANSYS analysis in the present study. The main reason for the slight difference is the type of brace's connection to the beam-column. In ANSYS models, it was not possible to generate a perfect hinge, whereas the connections in the models of Ghassemiyeh and Kari (2008) were considered as perfect hinges. The details of brace's connection to the beam-column in the ANSYS models are described below. The connection between the beam and column was considered as a perfect hinge.

In an ordinary case, the PGA of El-Centro earthquake is 0.3*g*. Under this acceleration, the response of a structure remains linear and, consequently, there was no difference between the behaviour of different models. The probable reason for this could be that the behaviors of steel and SMA in the linear region are identical. Hence, in the present research, El-Centro earthquakes with PGAs of 0.6*g* and 0.9*g* were used to ensure that the behavior of brace would enter the nonlinear region.

- ***Model specifications***

The studied structure is the same three-story structure proposed by Sabelli, which was explained above. The difference in these structures is that the behavioral model of alloys is different. Six types of hybrid bracing were used in this investigation in which the longitudinal consumption percentage of SMA was 0, 20, 40, 60, 80, and 100. In fact, the first model was composed of steel only and the last one was composed of only SMA.

The percentage content of steel and the SMA in the braced frames and their schematics are shown in Table 3 and Figure 11, respectively.

Table 3. The percentage content of steel and SMA used in bracings

Model Number	The Percentage of The SMA Consumption	The Percentage of Steel Consumption
1st model	0	100
2nd model	20	80
3rd model	40	60
4th model	60	40
5th model	80	20
6th model	100	0

Fig. 11. The schematic depiction of steel–SMA hybrid brace

The behavioral model of steel and SMA used in the studied hybrid braces is illustrated in Figure 12 and Table 4. As observed in Figure 12, the nonlinear slope of SMA and steel were probably identical. This observation implies that the area under the stress-strain curve for SMA and steel was probably equal.

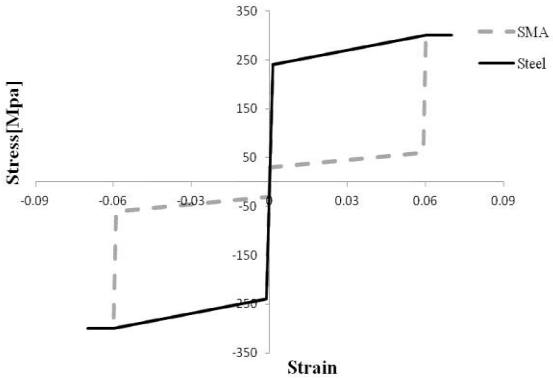

Fig. 12. The stress−strain diagram of steel and SMA used in bracings

Table 4. Parameters used in the behavioral model of SMA (Kazemi-Choobi et al., 2012)

Parameter	Definition	Value
σ_s^{AS}	Stress related to the beginning of the direct transformation phase	240 MPa
σ_f^{AS}	Stress related to the end of the direct transformation phase	300 MPa
σ_s^{SA}	Stress related to the beginning of the reverse transformation phase	60 MPa
σ_f^{SA}	Stress related to the end of the reverse transformation phase	30 MPa
ε_L	Maximum strain caused by phase transformation	6%
Y_{mrt}	Modulus of martensite	80000 MPa

Solid 185 elements were used for the modeling of the frame. Due to the use of solid elements, it was difficult to generate a perfect hinge at the junction of the brace and the beam-column. This caused an additional force at the corners of the bracings. The models generated and meshed in the ANSYS are shown in Figures 13 and 14.

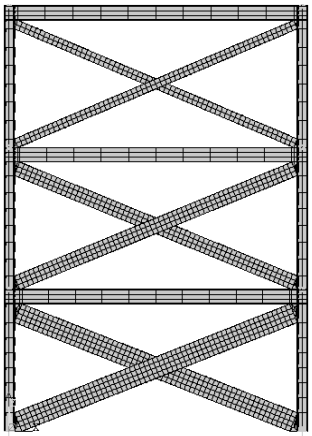

Fig. 13. The modeling of the frame in ANSYS

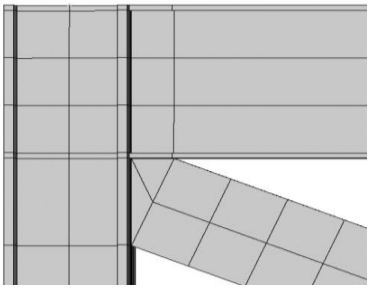

Fig. 14. The modeling of the connection between the brace and the beam-column

RESULTS AND DISCUSSION

Two major differences were noted between the behavior of steel and SMA, i) the SMA can return to its original state after bearing large strains and to minimize the horizontal displacement of structure and ii) the energy absorption of the structure was increased. The area under the force–displacement curve was followed to calculate the energy in a cumulative fashion.

This section attempts to provide the optimum design for the brace by comparing the time histories of horizontal displacement and the diagrams of structural energy absorption in all models in terms of both SMA consumption and the seismic performance.

Comparison of the Residual Horizontal Displacement and the Energy Absorption

Time histories of the horizontal displacement at the level of third floor under the maximum acceleration of 0.6*g* are shown in Figures 15-20.

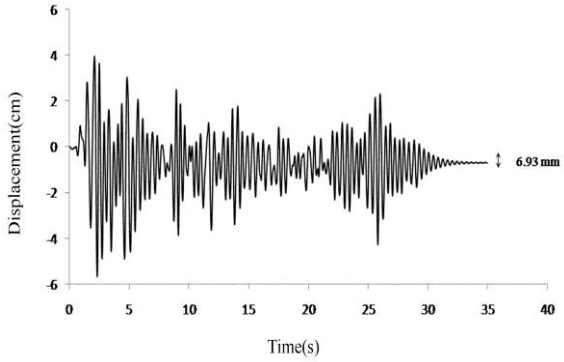

Fig. 15. Time history of the horizontal displacement at the level of third floor in a bracing system with a combination of 0% SMA and 100% steel under the maximum acceleration of 0.6g

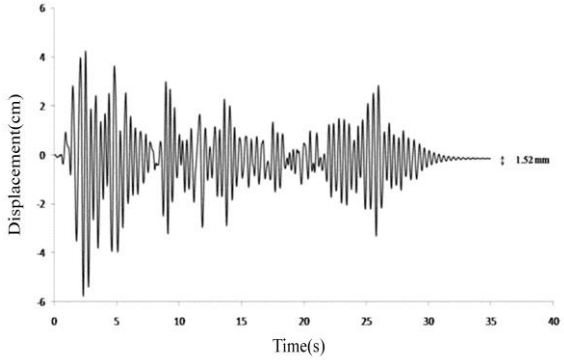

Fig. 16. Time history of the horizontal displacement at the level of third floor in a bracing system with a combination of 20% SMA and 80% steel under the maximum acceleration of 0.6g

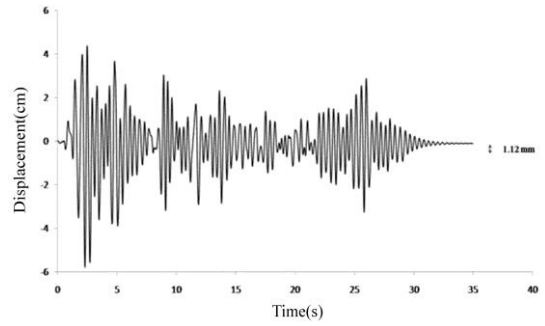

Fig. 17. Time history of the horizontal displacement at the level of third floor in a bracing system with a combination of 40% SMA and 60% steel under the maximum acceleration of 0.6g

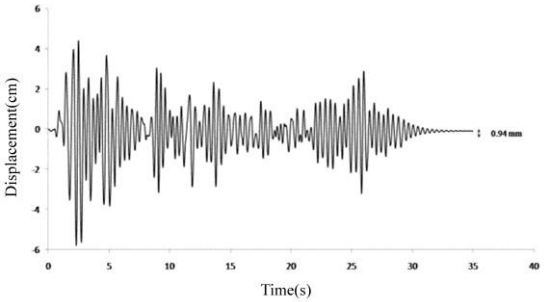

Fig. 18. Time history of the horizontal displacement at the level of third floor in a bracing system with a combination of 60% SMA and 40% steel under the maximum acceleration of 0.6g

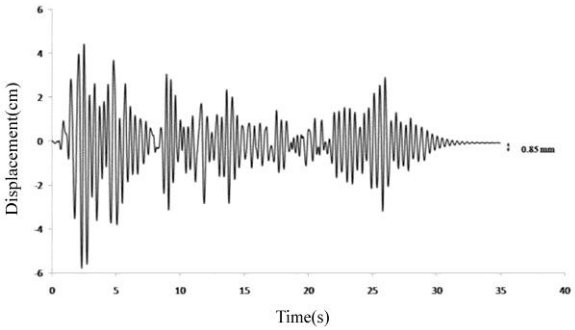

Fig. 19. Time history of the horizontal displacement at the level of third floor in a bracing system with a combination of 80% SMA and 20% steel under the maximum acceleration of 0.6g

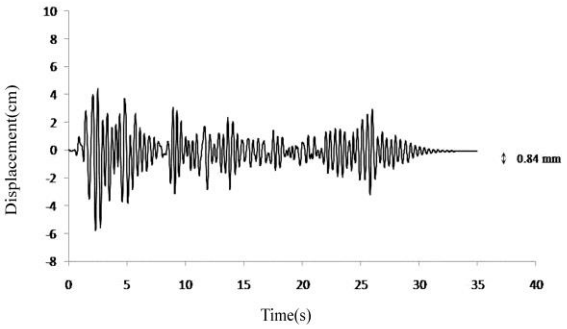

Fig. 20. Time history of the horizontal displacement at the level of third floor in a bracing system with a combination of 100% SMA and 0% steel under the maximum acceleration of 0.6g

For a better comparison, the values of the residual displacement of structure under the maximum acceleration of 0.6 *g* are given in Table 5 and Figure 21. The results of energy absorption are presented in Table 6 and in Figure 22. The *DOD* and *DOE* mentioned in Figures 21 and 22 were calculated according to Eqs. (1) and (2).

DOD is a measure of comparison of residual displacements in the hybrid bracing system with a specific amount of steel and SMA with full-steel and full-SMA braces.

$$DOD = (D_M - D_{ST})/(D_{SMA} - D_{ST}) \qquad (1)$$

where D_M: is the residual displacement in the hybrid bracing system, and D_{ST} and D_{SMA}: are the residual displacements in full-steel and full-SMA braces, respectively.

Table 5. The comparison of the residual displacement of structure in the studied bracing systems under the maximum acceleration of 0.6g

Bracing System	Residual Displacement of Structure (mm)	DOD (%)
0% SMA and 100% Steel	6.93	0%
20% SMA and 80% Steel	1.52	89%
40% SMA and 60% Steel	1.12	95%
60% SMA and 40% Steel	0.94	98%
80% SMA and 20% Steel	0.85	99.9 %
100% SMA and 0% Steel	0.84	100 %

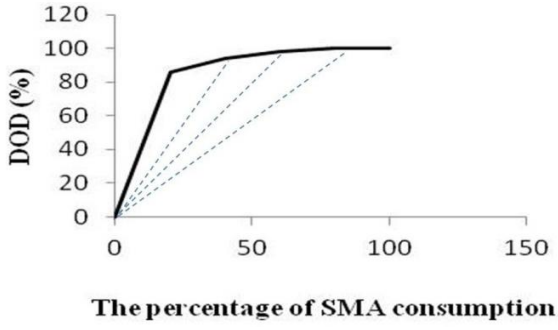

Fig. 21. Comparison of SMA consumption with the DOD under the maximum acceleration of 0.6g

DOE is the measure of comparison of energy absorption in the hybrid bracing system with a specific amount of steel and SMA with full-steel and full-SMA braces.

$$DOE = (E_M - E_{ST})/(E_{SMA} - E_{ST}) \qquad (2)$$

where E_M: is the value of structural energy absorption in the hybrid bracing system, and E_{ST} and E_{SMA}: are the values of structural energy absorption in full-steel and full-SMA braces, respectively.

Table 6. The comparison of the value of structural energy absorption in the bracing systems under the maximum acceleration of 0.6g

Bracing System	Value of Energy Absorption (kN.m)	DOE (%)
0% SMA and 100% Steel	453	0
20% SMA and 80% Steel	455	41
40% SMA and 60% Steel	456	66
60% SMA and 40% Steel	456.4	76
80% SMA and 20% Steel	457.4	99
100% SMA and 0% Steel	457.5	100

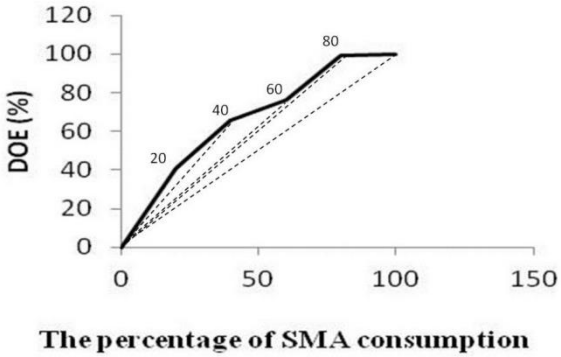

Fig. 22. Comparison of SMA consumption with the DOE under the maximum acceleration of 0.6g

According to Figures 21 and 22 and by comparing the results of hybrid braces with the results of full-steel (1st model) and full-SMA (6th model) braces, it can be observed that the increase in SMA consumption improves the seismic performace. However, considering the major difference between the cost of steel and SMA, the present paper aimed to determine the optimal amount of SMA to be used along with steel in a hybrid brace such that a compromise is formed between the brace cost and its seismic performance. Based on Figures 21 and 22, this optimal state is achieved when the slope of the

curve with respect to the origin of the coordinate system is steep. This is because, I under such a condition, SMA consumption is relatively low, while the seismic performance of the bracing system is considerably enhanced.

Figure 22 depicts that the amount of energy absorption in various models were not considerably different. This is because, under the maximum acceleration of 0.6 *g*, the behavior of models during the earthquake was mainly linear; and nonlinear behavior was detected only in short durations. As the linear behaviors of steel and SMA are the same,the amount of energy absorption in various models are not considerably different. To indicate this behavior more clearly, the hystersis curves for full-SMA (6^{th} model) and full-steel (1^{st} model) braces have been shown in Figures 23 and 24, respectively.

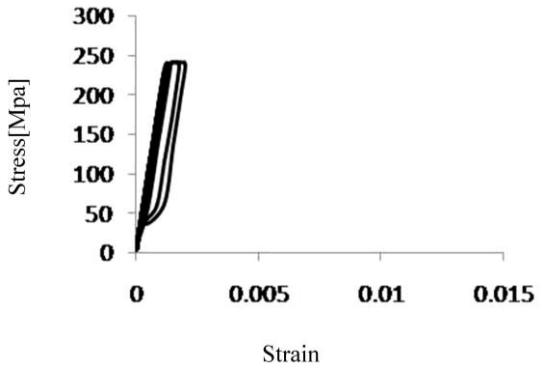

Fig. 23. Hysteresis graph of the SMA bracing (6th model) under the maximum acceleration of 0.6g

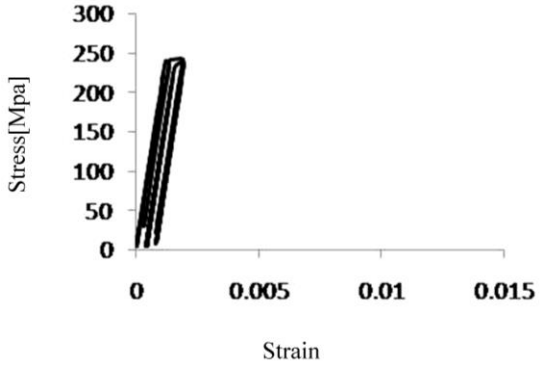

Fig. 24. Hysteresis graph of steel bracing (1^{st} model) under the maximum acceleration of 0.6g

As mentioned earlier, models were investigated under the maximum accelerations of 0.6*g* and 0.9 *g*. The results of the models under the maximum acceleration of 0.9*g* are presented in Tables 7 and 8 and in Figures 25−27.

Table 7 displays the results of residual structural displacement under the maximum acceleration of 0.9 *g*; and Figure 25 depicts the SMA consumption versus the value of residual structural displacement in the considered models under the maximum acceleration of 0.9*g*. In Figure 26 and Table 8, the structural energy absorption was compared between the bracing systems for the maximum acceleration of 0.9*g*; and Figure 27 compares the percentage of SMA consumption with the *DOE* under this level of acceleration.

Table 7. Comparison of the residual structural displacement in the studied bracing systems under the maximum acceleration of 0.9 g

Bracing System	Residual Structural Displacement (mm)	DOD (%)
0% SMA and 100% steel	35.93	0
20% SMA and 80% steel	2.14	96.8
40% SMA and 60% steel	1.71	98
60% SMA and 40% steel	1.18	99
80% SMA and 20% steel	1.06	99.8
100% SMA and 0% steel	1.01	100

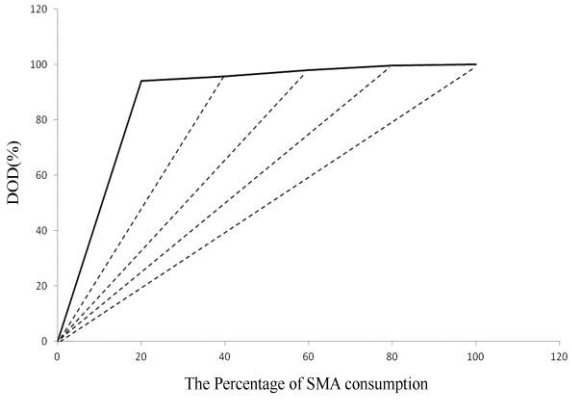

Fig. 25. DOD versus SMA consumption percentage under the maximum acceleration of 0.9 g

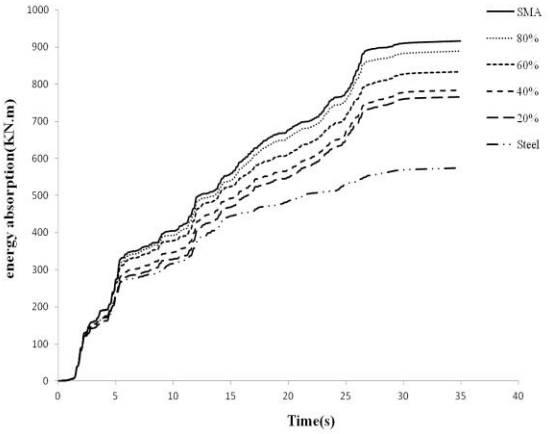

Fig. 26. Comparison of the graphs of structural energy absorption in the studied bracing systems under the maximum acceleration of 0.9 g

Table 8. Comparison of the value of structural energy absorption in the studied bracing systems under the maximum acceleration of 0.9 g

Bracing System	Value of Energy Absorption (KN.m)	DOE (%)
0% SMA and 100% steel	552	0
20% SMA and 80% steel	753	55
40% SMA and 60% steel	776.2	61.5
60% SMA and 40% steel	796.8	67
80% SMA and 20% steel	884	91
100% SMA and 0% steel	917	100

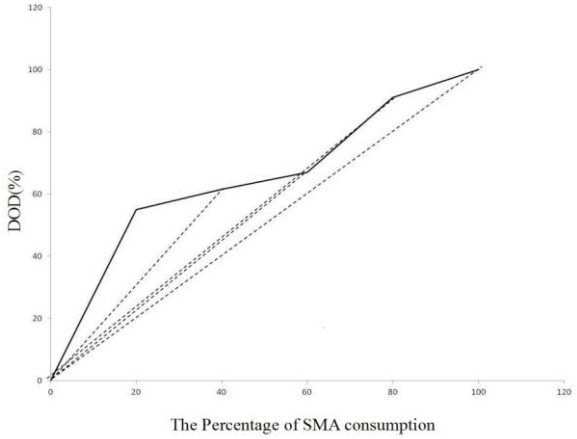

Fig. 27. DOE versus the SMA consumption percentage under the maximum acceleration of 0.9 g

As shown in Figures 21, 22, 25, and 27, it can be concluded that a bracing system composed of 20% SMA and 80% steel is the optimal steel-SMA hybrid brace. In this hybrid brace, with SMA consumption of only 20%, the values of *DOD* are 96.8% (maximum), 41% (minimum), 89%, and 55%, respectively.

In the present study, the stress–strain diagram introduced for steel was, in some aspects, similar to that of SMA. One of their most important similarities was the energy absorption in the first loop. As shown in the stress–strain diagram in Figure 12, these two materials have almost identical energy absorption pattern. However, in the studied models, increasing the consumption of SMA leads to an increase in energy absorption and, with the increase in the intensity of the earthquake, this behavior becomes even more evident. The main reason for this special behavior of the SMAs, that is, returning to the original state after unloading and resistance to the fatigue. These differences can be clearly observed in the hysteresis diagrams of steel and SMA braces under the maximum acceleration of 0.9 *g* (Figures 28 and 29).

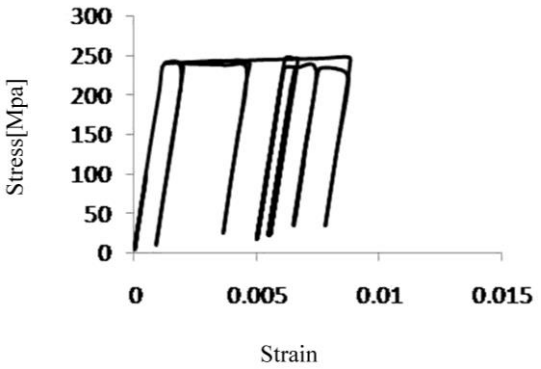

Fig. 28. Hysteresis diagram of full-steel brace (1st model) under the maximum acceleration of 0.9 g

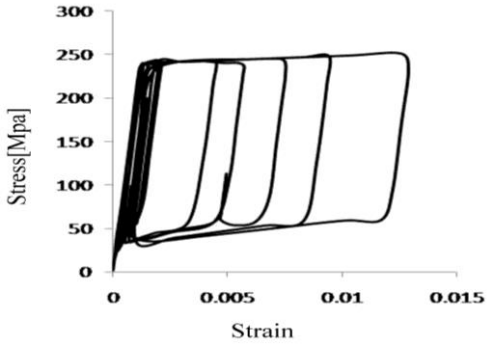

Fig. 29. Hysteresis diagram of full-SMA brace (6th model) under the maximum acceleration of 0.9 g

CONCLUSIONS

In the present study, the stress-strain diagram introduced for steel was similar to that of SMA. One of the most important similarities between the two diagrams was the energy absorption in the first loop. However, in the studied models, increasing the SMA content led to a subsequent increase in the energy absorption; with an increase in the intensity of earthquake, this behavior became more evident. The main reason for this is the special behavior of SMAs, i.e., returning to the initial state after unloading.

The optimum SMA-steel combination for the hybrid bracing system was found to be 20% SMA and 80% steel, in which, which gave a minimum performance of 41% and a maximum performance of 96.8% in comparison with 100% SMA-0% steel combination.

The seismic performance of SMA-steel hybrid braces was not significantly different from that of steel braces under weak and moderate earthquakes (say, the maximum acceleration of 0.6*g*). Thus, using SMAs in braces is not economically justifiable for improving the seismic performance against weak and moderate earthquakes.

ACKNOWLEDGMENT

The authors express their deepest appreciations to the three anonymous reviewers who reviewed and provided their valuable comments on the draft version of this paper.

REFERENCES

Alvandi, S. and Ghassemieh, M. (2014). "Application of shape memory alloys in seismic isolation: A review", *Civil Engineering Infrastructures Journal*, 47(2), 153-171.

Asgarian, B. and Moradi, S. (2011). "Seismic response of steel braced frames with shape memory alloy braces", *Journal of Constructional Steel Research*, 67(1), 65-74.

Auricchio, F., Fugazza, D. and Desroches, R. (2006). "Earthquake performance of steel frames with Nitinol braces", *Earthquake Engineering*, 10(1), 45-66.

Ben Mekki, O. and Auricchio, F. (2011). "Performance evaluation of shape-memory-alloy superelastic behavior to control a stay cable in cable-stayed bridges", *International Journal of Non-Linear Mechanics*, 46(2), 470-477.

Ghassemiyeh, M. and Kari, A. (2008). "Comparison of the Seismic Performance Improvement in the Structures with braces made of SMA and Buckling-Restrained Braces (BRB)", *4th National Congress of Civil Engineering*, Tehran, Iran.

Kazemi-Choobi, K., Khalil-Allafi, J. and Abbasi-Chianeh, V. (2012). "Investigation of the recovery and recrystallization processes of Ni50.9Ti49.1 shape memory wires using in situ electrical resistance measurement", *Materials Science Engineering A*, 551(15), 122-127.

Ma, H. and C.H.Yam, M. (2011). "Modelling of a self-centering damper and its application in structural control", *Journal of Constructional Steel Research*, 67(4), 656-666.

Malagisi, S., Marfia, S., Sacco, E. and Toti, J. (2014). "Modeling of smart concrete beams with shape memory alloy actuators", *Engineering Structures*, 75(1), 63-72.

Mansouri, A. (2008). *Investigating the behavior factor of concrete frames braced with SMAs*, M.Sc. Thesis, Faculty of Civil Engineering, University of Tabriz, (in Persian).

Miller, D.J., Fahnestock, L.A. and Eatherton, M.R. (2012). "Development and experimental validation of a nickel–titanium shape memory alloy self-centering buckling-restrained brace", *Engineering Structures*, 40(1), 288-298.

Motahari, S.A., Ghassemiyeh, M. and Abolmaali, S.A. (2007). "Implementation of shape memory alloy dampers for passive control of structures subjected to seismic excitations", *Journal of Constructional Steel Research*, 63(12), 1570-1579.

Muntasir Billah, A.H.M. and Shahria Alam, M. (2012). "Seismic performance of concrete columns reinforced with hybrid shape memory alloy (SMA) and fiber reinforced polymer (FRP) bars", *Construction and Building Materials*, 28(1), 730-742.

Ozbulut, O.E. and Hurlebaus, S. (2011). "Energy-balance assessment of shape memory alloy-based seismic isolation devices", *Smart Structures and Systems*, 8(4), 399-412.

Padgett, J., Desroches, R. and Ehlinger, R. (2009). "Experimental response modification of a four-span bridge retrofit with shape memory alloys",

Structural Control and Health Monitoring, 17(6), 694-708.

Sabelli, R. (2001). *Research on improving the design and analysis of earthquake-resistant steel-braced frame*, Professional Fellowship Report No. PF2000-9, NEHRP, US.

Shrestha, K.C. et al., (2011). "Applicability of Cu-Al-Mn shape memory alloy bars to retrofitting of historical masonry constructions", *Smart Structures and Systems*, 3(2), 233-256.

Speicher, M.S., Des Roches, R. and Leon, R.T. (2011). "Experimental results of a NiTi shape memory alloy (SMA)-based recentering beam-column connection", *Engineering Structures*, 33(9), 2448-2457.

Sun, W. (2011). "Seismic response control of high arch dams including contraction joint using nonlinear super-elastic SMA damper", *Construction and Building Materials*, 25(9), 3762-3767.

Walter Yang, Ch.Sh., Desroches, R. and Leon, R.T. (2010). "Design and analysis of braced frames with shape memory alloy and energy-absorbing hybrid devices", *Engineering Structures*, 32(2), 498-507.

Yam, M.C.H., Fang, C., Lam, A.C.C. and Zhang, Y. (2014). "Numerical study and practical design of beam-to-column connections with shape memory alloys", *Journal of Constructional Steel Research*, 104(1), 177-192.

Youssef, M.A. and Elfeki, M.A. (2012). "Seismic performance of concrete frames reinforced with superelastic shape memory alloys", *Smart Structures and Systems*, 9(4), 313-333.